Probing α-Helical Secondary Structure at a Specific Site in Model Peptides via Restriction of Tryptophan Side-Chain Rotamer Conformation

K. J. Willis,[‡§] W. Neugebauer,[§] M. Sikorska,[§] and A. G. Szabo[§]

[‡]Allelix Biopharmaceuticals Inc., Mississauga, Ontario, Canada L4V 1P1, and [§]The Institute for Biological Sciences, National Research Council, Ottawa, Ontario, Canada K1A 0R6

ABSTRACT The relationship between α-helical secondary structure and the fluorescence properties of an intrinsic tryptophan residue were investigated. A monomeric α-helix forming peptide and a dimeric coiled-coil forming peptide containing a central tryptophan residue were synthesized. The fluorescence parameters of the tryptophan residue were determined for these model systems at a range of fractional α-helical contents. The steady-state emission maximum was independent of the fractional α-helical content. A minimum of three exponential decay times was required to fully describe the time-resolved fluorescence data. Changes were observed in the decay times and more significantly, in their relative contributions that could be correlated with α-helix content. The results were also shown to be consistent with a model in which the decay times were independent of both α-helix content and emission wavelength. In this model the relative contributions of the decay time components were directly proportional to the α-helix content. Data were also analyzed according to a continuous distribution of exponential decay time model, employing global analysis techniques. The recovered distributions had "widths" that were both poorly defined and independent of peptide conformation. We propose that the three decay times are associated with the three ground-state χ_1 rotamers of the tryptophan residue and that the changes in the relative contributions of the decay times are the result of conformational constraints, imposed by the α-helical main-chain, on the χ_1 rotamer populations.

INTRODUCTION

It is frequently desirable to be able to determine the structure and dynamics of proteins or polypeptides at a specific site. In the case of small flexible peptides this information may be important in, for example, studies of protein folding or in the design of peptide ligands. NMR spectroscopy can be used to define the solution conformation of peptides (Dyson and Wright, 1991). Fourier transform infrared (FTIR) spectroscopy (Krimm and Bandekar, 1986) and circular dichroism (CD) spectroscopy (Woody, 1985) have also been applied extensively in secondary structure analysis. However, CD cannot readily provide information on the conformation at a specific position and this limitation also applies to FTIR, unless isotopic labels are introduced (Tadesse et al., 1991).

Tryptophan residues have been used as intrinsic, site specific, fluorescence probes of structure and dynamics in a large number of studies (Eftink, 1991). The fluorescence properties of a tryptophan residue potentially report on the "local" structure and environment. Unfortunately, the relationship between the measurable fluorescence parameters and the secondary structure in the region of the tryptophan residue have not been clearly established. Recently however, time-resolved fluorescence spectroscopy was used in an attempt to assign an α-helical or random coil main-chain conformation to a segment of a peptide hormone containing a tryptophan residue (Willis and Szabo, 1992).

Peptides of de novo design can be synthesized that display significant α-helical secondary structure in aqueous solution (Scholtz and Baldwin, 1992). Such peptides, containing a single tryptophan residue, represent a useful model system for systematically correlating fluorescence emission and secondary structure. In this report we describe the results of unfolding experiments on the fluorescence properties of a tryptophan residue located in the center of two model α-helical peptides.

The first model peptide is based on a "leucine zipper" sequence reported by O'Neil and DeGrado (1990) which in solution exists in an equilibrium between nonhelical monomers and parallel α-helical dimers. A central substitution site is present in the sequence which is solvent exposed, and not in direct contact with the dimerization surface of the coiled-coil dimer. Helix formation in this model is essentially a two-state process and can be investigated simply by varying the peptide concentration. The second model peptide forms a monomeric α-helix stabilized by glutamate/lysine ion pairs and was adapted for our purposes from a sequence designed by Marqusee and Baldwin (1987).

MATERIALS AND METHODS

Peptide preparation

Peptides were synthesized using fluoren-9-ylmethoxycarbonyl (FMOC) protected amino acids on a Rink amide support (Fields and Noble, 1990;

Received for publication 24 November 1993 and in final form 15 February 1994.

Address reprint requests to Arthur G. Szabo, Department of Chemistry and Biochemistry, University of Windsor, 401 Sunset, Windsor, Ontario N9B 3P4 Canada. Tel.: 519-253-4232 (ext. 3526); Fax: 519-973-7098; E-Mail: szabo@server.uwindsor.ca.

Dr. Willis' present address: Procept Inc., 840 Memorial Dr., Cambridge, MA 02139 USA.

Dr. Szabo's present address: Department of Chemistry and Biochemistry, University of Windsor, Windsor, Ontario N9B 3P4 Canada.

Abbreviations used: CD, circular dichroism; FMOC, fluoren-9-ylmethoxycarbonyl; FTIR, Fourier transform infrared; GuHCl, guanidinium hydrochloride; HD, helical dimer peptide; HM, helical monomer peptide; NMR, nuclear magnetic resonance; TFA, trifluoroacetic acid; SVR, serial variation ratio.

0006-3495/94/05/1623/08 $2.00

Rink, 1987; Sieber, 1987). Coupling was carried out according to Knorr et al. (1989) and Bernatowicz et al. (1989). Reagents were products of Amino-Tech (Ottawa, Ont., Canada). The following side chain protecting groups were used, Lys: tert-butoxycarbonyl; His, Gln: trityl; Glu: t-butyl ester. Peptides were acetylated with 50% acetic anhydride in piperidine and cleaved from the resin with 95% trifluoroacetic acid (TFA) according to Bernatowicz et al. (1989). The crude peptides were purified by reversed-phase HPLC on a C_{18} column with 0.1% aqueous TFA/0.1% TFA acetonitrile. Final products were analyzed by analytical reversed-phase HPLC and mass spectrometry employing nebulization-assisted electrospray ionization (API III quadrupole. Sciex, Mississauga, Ont., Canada) from a 0.5 mg/mL solution in 10% HOAc.

Circular dichroism spectroscopy

CD measurements were made with a JASCO 6000 spectropolarimeter at 20°C. The instrument was calibrated with aqueous *d*-10-camphorsulfonic acid. Peptide concentration in 1 mM phosphate buffer, pH 7.5, was determined from the absorbance at 280 nm using an extinction coefficient of 5559 M^{-1} cm^{-1}. Elipticity is reported as mean residue molar elipticity.

Fluorescence spectroscopy

Steady-state fluorescence measurements at 20°C and a spectral resolution of 4 nm, were made on an SLM 8000 C spectrofluorimeter in the ratio mode, with polarizers oriented to eliminate anisotropy effects. Corrections were made for the (negligible) signal from a buffer blank and for the wavelength dependence of the instrument response.

Time resolved fluorescence data were collected at 20°C using the technique of time-correlated single photon counting with laser/microchannel plate based instrumentation (Willis and Szabo, 1989). The excitation wavelength was 295 nm, and emission was detected, after passing through a polarizer set at 55° to the vertical, at wavelengths in the range 310–420 nm with a band-pass of 4 nm. The channel width was 10 ps, and data were collected in 2048 channels. An instrument response function was determined from the Raman scattering of the excitation (Willis et al. 1990), by water at 328 nm and had a fwhm of 60 ps. Each decay curve typically contained (1–2) $\times$ 10^6 total counts and corrections were made for the signal from a buffer blank (usually negligible).

Two models were fitted to the data. The function describing the fluorescence intensity decay following δ-function excitation was assumed to be a sum of exponentials (discrete component analysis) or alternatively a sum of γ probability densities (continuous γ distribution analysis) as described earlier (Willis et al., 1990b). Procedures for the simultaneous or "global" (Knutson et al., 1983) analysis of multiple time-resolved data sets and criteria for assessing the quality of the fit of the model to the data are given elsewhere (Willis and Szabo, 1989).

In the case of the discrete component analysis, the emission spectrum associated with each decay time, and presumably therefore, each ground-state species (DAS, decay-associated spectra; Knutson et al., 1982) were determined and used to derive the fractional concentration of each ground-state species, c_i,[1] as previously described (Willis and Szabo, 1992).

RESULTS

Peptides

Two α-helical model peptides with a centrally located tryptophan residue were synthesized. An α-helical dimer forming peptide designated HD (Ac-E-L-E-A-L-E-K-K-L-A-A-L-E-*W*-K-L-Q-A-L-E-K-K-L-E-A-L-E-H-G-amide), and a monomeric α-helix forming peptide designated HM (Ac-A-E-A-A-A-K-E-A-*W*-A-K-E-A-A-A-K-A-amide). HD differs by a single substitution (W2L) from a sequence, containing a central tryptophan residue, reported earlier (O'Neil and DeGrado, 1990) to exist in an equilibrium between non-helical monomers and α-helical dimers. A monomeric peptide, which has been shown to exhibit a significant population of helical residues in solution (Marqusee and Baldwin, 1987), was modified by substitution of a tryptophan at the central 9 position (A9W: see Merutka et al., 1990) to give the HM sequence. The purity and identity of both HD and HM were established by analytical reverse-phase HPLC and mass spectrometry. The expected molecular weights of 3373 (HD) and 1728 (HM) were found with mass spectra composed predominantly of the +3 to +6 and +1 to +3 protonated molecular ions, respectively. These results are consistent with the expected sequence of each peptide.

Circular dichroism

The CD spectra of HD at μM concentrations indicated a high helical content, and as expected (O'Neil and DeGrado, 1990) showed a concentration dependence consistent with a (non-helical) monomer (100% helical) dimer equilibrium (Fig. 1). Dissociation in the spectroscopically convenient 1–100 μM concentration range, was facilitated by the denaturant guanidinium hydrochloride (GuHCl) at 2.4 M. Addition of GuHCl to a fixed concentration of the peptide resulted in changes in the CD spectra similar to those observed on decreasing the peptide concentration, consistent with the dis-

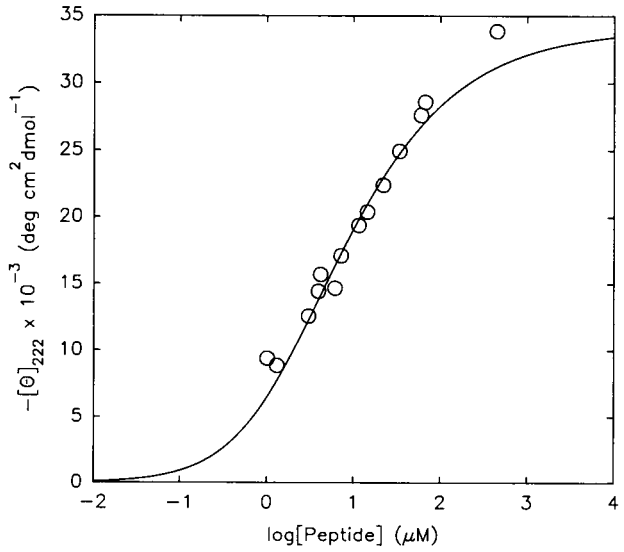

FIGURE 1 Dependence of the mean residue molar ellipticity at 222 nm on peptide concentration for the α-helical dimer forming model peptide. Peptide was dissolved in 1 mM phosphate, pH 7.5 containing 2.4 M GuHCl. The solid line represents a fit to a monomer-dimer equilibrium in which $[\Theta]_{222}$ (monomer) = 0, $[\Theta]_{222}$ (dimer) = −34,000, and the equilibrium constant = 7 μM.

[1] In this paper c_i is the (emission wavelength independent) fractional concentration of each ground-state species, as defined in Willis and Szabo, 1992. In Willis et al., 1990b the symbol $c_i(\lambda)$ was used to designate a different set of parameters, namely the linear factors that describe the relative contributions of the multiple modes in the continuous γ distribution analysis.

sociation of the α-helical dimer to form nonhelical monomer (data not shown).

HM peptide exhibited CD properties analogous to those reported earlier for peptides of closely similar sequence (Marqusee and Baldwin, 1987; Merutka et al., 1990, 1991; Merutka and Stellwagen, 1991) and indicated ~30% helical structure at 20°C. This helical structure, which was independent of peptide concentration in the μM range, was destabilized by the addition of GuHCl as assessed by the reduction in elipticity at 222 nm (data not shown).

Steady-state fluorescence

Fluorescence spectra, excited at 295 nm, of both HD and HM were characteristic of a solvent exposed tryptophan residue, having an emission maximum of 351 ± 2 nm. The emission maximum was independent of [peptide] (1–400 μM) and [GuHCl] (0–6 M). This suggests that neither dimerization (HD) nor the helix/coil transition (HD and HM), alter the hydrophobicity of the central tryptophan residues environment. [The central substitution site in HD is not in direct contact with the dimerization surface of the coiled-coil (O'Neil and DeGrado, 1990)].

Time-resolved fluorescence

Data were collected for HD at a series of peptide concentrations to sample the nonhelical monomer/α-helical dimer equilibrium. For each sample the fluorescence decay was measured at least at ten different emission wavelengths across the fluorescence spectrum. Analysis of each of the individual data sets showed that the decay times were constant across the spectrum for a given sample. The χ^2 values for the individual datasets ranged from 1.02 to 1.05. Hence these individual data sets could be combined in a global analysis. The results are summarized in Fig. 2. At each of seven peptide concentrations a global analysis of multiple emission wavelength data, assuming three emission wavelength independent discrete exponential decay times (τ_i), gave an excellent fit to the data ($1.03 \leq \chi^2 \leq 1.07$ and $1.82 \leq \text{SVR} \leq 1.97$). In contrast discrete bi-exponential decay models gave comparatively poor fits to the data, with $1.37 \leq \chi^2 \leq 1.17$ and $1.13 \leq \text{SVR} \leq 1.55$. The normalized preexponential terms (α_i) recovered from the triple exponential analysis performed at each peptide concentration, also showed little wavelength dependence. Consequently the decay associated emission spectra were of similar shape and the calculated (emission wavelength independent) c_i parameters (Willis and Szabo, 1992) were approximately equal to the α_i (λ).

Transition from the nonhelical to the helical state, apparently resulted in an approximately 35% increase in both the long and intermediate decay time values, while the short decay time was unchanged. The fractional concentration of the long decay time increased by 50% while those of the intermediate and short decay times decreased by 20% (Fig.2). However, the quality of the fit of a discrete triple exponential model, did not deteriorate at intermediate peptide concentrations where both conformations were significantly populated.

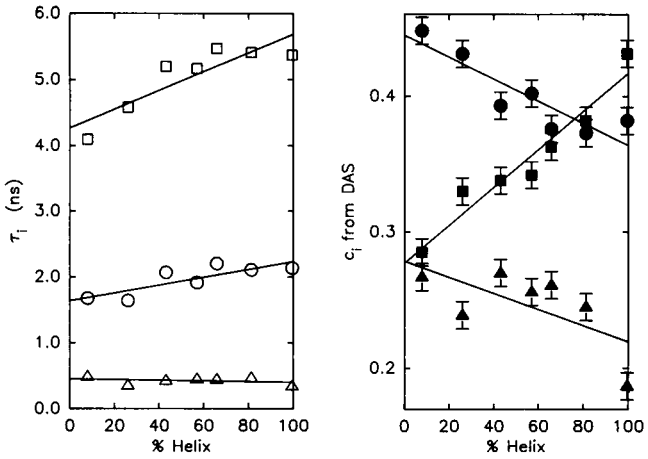

FIGURE 2 Dependence of the time-resolved fluorescence decay parameters on the % α-helix, for the α-helical dimer forming peptide (HD). Measurements were made at peptide concentrations in the range 1–400 μM in the presence of 2.4 M GuHCl (for the first point 3.8 M GuHCl was used), and helix content was determined by CD (see Fig. 1). The excitation wavelength was 295 nm. Fluorescence parameters, recorded at *each* % α-helix, represent the results of a global fit to 11 data sets collected as a function of emission wavelength (310–420 nm). The same emission wavelengths were used in each case, and individual data sets contained 1 to 2×10^6 total counts in 2048 channels. Fluorescence decay times (τ_i) have standard errors, as determined from the nonlinear least-squares analysis, within the contours of the plotted symbols. The *squares, circles,* and *triangles* represent the long, intermediate, and short decay times, respectively. Corresponding filled symbols represent the (emission wavelength-independent) fractional concentrations (c_i) associated with each decay time component class. Solid lines represent the straight line that best fits the data in each case.

Distribution model

Data which yield excellent fit statistics to a discrete exponential decay model can also be equally well described by a model in which a continuous distribution of exponential decays is assumed (James and Ware, 1985; Alcala et al., 1987; Bayley and Martin, 1989). The width of the recovered distribution is reported to reflect the heterogeneity of the tryptophan residues microenvironment in a protein, increasing on denaturation and displaying a maximum at the midpoint (Mei et al., 1992). Table 1 summarizes the results of a trimodal continuous γ distribution analysis (Willis et al., 1990b) of the data for the fully helical HD peptide. Ten data sets collected at a series of emission wavelengths and a fixed peptide concentration (400 μM) were analyzed simultaneously.

When we attempted to fit a single γ distribution or a bimodal γ distribution model to these data poor fits were obtained. The nonlinear least-squares minimization failed to converge when a trimodal γ distribution analysis was performed. Constraining the mean decay times of the three modes of the distribution to the values recovered from a discrete triple exponential model (Fig. 2) also did not allow the analysis to converge. This indicated that the quality of the

TABLE 1 Trimodal continuous γ distribution analysis of α-helical dimer fluorescence decay data

Constrained value of σ_i‡	HW_1§	HW_2	HW_3	χ^2	SVR
	ns	ns	ns		
k_i^*	6.3	2.4	0.35	1.70	0.73
$k_i^*/2$	3.1	1.2	0.18	1.10	1.74
$k_i^*/2.5$	2.5	1.0	0.14	1.08	1.79
$k_i^*/3$	2.1	0.8	0.12	1.07	1.82
$k_i^*/4$	1.6	0.6	0.09	1.07	1.83
$k_i^*/6$	1.1	0.4	0.06	1.07	1.82
$k_i^*/8$	0.8	0.3	0.04	1.07	1.84
$k_i^*/16$	0.4	0.2	0.02	1.07	1.83
$k_i^*/32$	0.2	0.1	0.01	1.07	1.83
Triexponential fit¶	-	-	-	1.07	1.83

** These data were for 400 μM α-helical dimer forming peptide in 1 mM phosphate, pH 7.5 containing 2.4 M GuHCl, and the helix content (by CD) was near 100%. Ten data sets collected as a function of emission wavelength (see Fig. 2) were analyzed using a global method (τ_i independent of λ_{em}).

‡ In the analysis, the SD of each of the three modes of the distribution (σ_i) was fixed at a given fraction of k_i^*; $k_i^* = 1/\tau_i$ where $\tau_1 = 5.37$ ns, $\tau_2 = 2.13$ ns, and $\tau_3 = 0.34$ ns, which are the decay times recovered by a triexponential fit to the data. All other parameters were unconstrained.

§ The approximate half-width at half-height of the distribution $HW_i = (2.1 \ln 2)^{1/2}\sigma_i/k_i 2$.

¶ Discrete, three component, global analysis.

fit was relatively insensitive to small variations in the standard deviations (σ_i; related to the width, see Table 1) of the modes of the distribution. If however, the standard deviations of the three modes were constrained the analysis converged and we were able to investigate the effect of distribution "width" on the quality of the fit and on the values of recovered parameters.

A distribution with three "narrow" modes (i.e. the ratio of the standard deviation to the mean was small) was found to give as good a fit to the data as a discrete triple exponential model, and the means of the distribution modes were centered on the discrete decay time values (Table 1). The mean decay times and the quality of the fit were insensitive to quite large increases in the width of the distribution modes. Similar results were obtained for the data collected at 11 μM peptide concentration (helix content 50%). For example, half widths of 2 ns were tolerated for the long decay time component without a significant change in the quality of the fit, despite employing a global analysis method.

While other distribution models may provide an apparent appropriate fit to the data, our experience has indicated that convergence of the fitting is difficult to obtain in most cases using either a continuous Gaussian or Lorentzian distribution. We conclude that for the system reported in this work, a discrete exponential model gives a fully satisfactory description of the fluorescence decay behavior.

Helix/coil independent decay times

It was clear that the discrete decay times associated with the helical and nonhelical states of the HD peptide were not sufficiently dissimilar and hence were not uniquely resolved. Indeed, we found that all the data were well described by a discrete triple exponential decay model in which the decay time components (τ_i) were independent of both emission wavelength *and* the α-helix content. This is illustrated by the data presented in Fig. 3 in which the helix content of a fixed concentration of the HD peptide was varied from 80% to 0% by the addition of GuHCl. [6 M GuHCl has negligible effects on the fluorescence properties of Trp model compounds (Willis and Szabo, 1992)]. Global analysis of the entire data set recovered three α-helix independent decay times of 5.80 ns, 2.73 ns, and 0.62 ns ($\chi^2 = 1.08$ for 16 data sets). On the other hand, it is significant that it was observed that the relative contributions of the three decay times showed a dramatic correlation with the α-helix content.

According to CD, 30% of the monomeric α-helix forming peptide HM was in the folded state in buffer. Time resolved fluorescence data were collected for HM at a series of concentrations of the denaturant GuHCl. They were well described by discrete triple exponential decay kinetics (Fig. 4). Recovered, % α-helix independent, decay times of 5.00 ns, 2.69 ns, and 0.73 ns ($\chi^2 = 1.04$ for 15 data sets) were similar to those for HD. The decay times were also independent of emission wavelength both in the presence (3 M) and absence of GuHCl (data not shown). A strong correlation of the relative contribution of the long and intermediate decay times

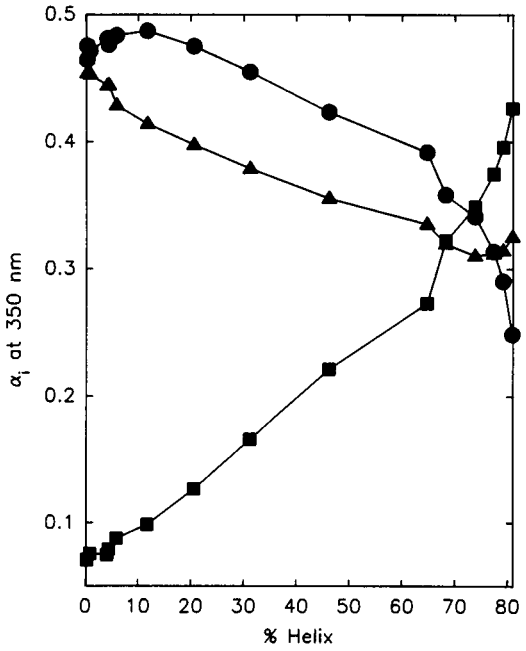

FIGURE 3 Dependence of the normalized preexponential term (α_i) associated with each decay time component, on the % α-helix, for the α-helical dimer forming peptide (HD). Measurements were made at a fixed peptide concentration of 4.2 μM in 1 mM phosphate, pH 7.5. The extent of helical dimer formation (by CD, see Fig.1) was varied by addition of GuHCl. Excitation was at 295 nm. Time-resolved fluorescence data were collected in 2048 channels (2×10^6 total counts) at 350 nm for 16 [GuHCl], over the range 0–6 M in 0.4 M steps. The squares, circles, and triangles represent the α_i (recovered from a global analysis) associated with % α-helix independent decay times of 5.80, 2.73, and 0.62 ns, respectively. The reduced χ^2 for the global fit was 1.08, and the SVR was 1.79. The solid lines have no significance.

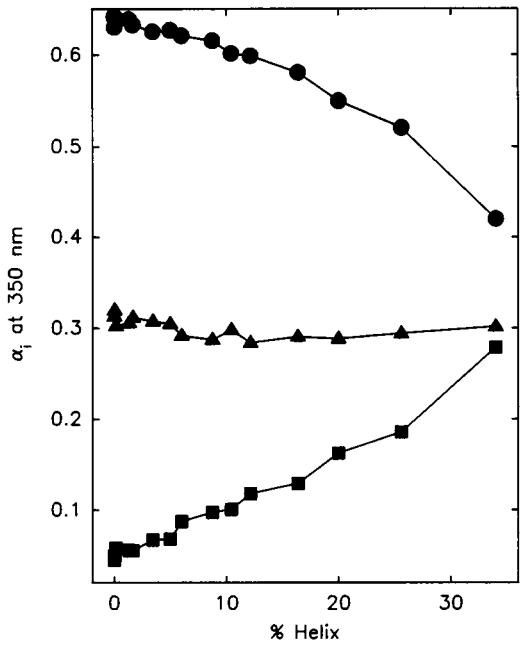

FIGURE 4 Dependence of the normalized preexponential term (α_i) associated with each decay time component, on the % α-helix, for the monomeric α-helix forming peptide (HM). Measurements were made at a fixed peptide concentration of 8.9 μM in 1 mM phosphate, pH 7.5. The extent of α-helix formation was determined by CD assuming $[\Theta]_{222}$ (100% helix) = −38,000 and $[\Theta]_{222}$ (0% helix) = −3000 deg cm^2 dmol^{-1} (Merutka et al., 1990) and was varied by addition of GuHCl. Excitation was at 295 nm. Time-resolved fluorescence data were collected in 2048 channels (2×10^6 total counts) at 350 nm for 15 [GuHCl], over the range 0–0.8 M in 57 mM steps. The squares, circles, and triangles represent the α_i (recovered from a global analysis) associated with % α-helix independent decay times of 5.00, 2.69, and 0.73 ns, respectively. The reduced χ^2 for the global fit was 1.04, and the SVR was 1.90. The solid lines have no significance.

with α-helix content was observed. However, the contribution of the short decay time remained essentially constant.

DISCUSSION

The side-chain of tryptophan can undergo rotation around the C_α-C_β and C_β-C_γ bonds defined by the angles[2] χ_1 and χ_2. In common with the side chains of other amino acids, the χ_1 distribution is trimodal and indicates a marked preference for the three fully staggered rotamers g^+ ($\chi_1 = 60°$), g^- ($\chi_1 = 60°$) and t ($\chi_1 = 180°$). Eclipsed rotamers are unfavorable due to steric clashes between the C_γ atom of the side-chain and the main chain C, N and O atoms. For aromatic amino acids two minimum energy conformations are found for the C_β-C_γ rotamers with $\chi_2 = 90°$ and $-90°$. These conformational preferences are supported by data from a variety of techniques including, for example, NMR (Ross et al., 1992), theoretical calculations (Piela et al., 1987; Gordon et al., 1992) and surveys of X-ray structures of proteins (Janin et al., 1978; Bhat et al., 1979; Benedetti et al., 1983; McGregor et al., 1987, Ponder and Richards, 1987; Schrauber et al., 1993).

Significantly there is a strong relationship between the side-chain conformation and secondary structure (Janin et al., 1978; Piela et al, 1987; McGregor et al., 1987; Schrauber et al., 1993). Clearly the main-chain peptide bonds attached to the α-carbon of a residue have different conformations (defined by the ϕ, Ψ dihedral angles) depending on the "local" secondary structure. The conformation of the main-chain peptide bonds influences χ_1 rotamer populations due to interactions with the C_γ atom.

Tryptophan and its simple derivatives generally display fluorescence decay kinetics more complex than a monoexponential decay law. For tryptophan residues triple exponential decays are typically required to model the time resolved data (Beechem and Brand, 1985; Eftink, 1991). This complexity is thought to originate primarily from the presence of χ_1 side-chain rotamers (Donzel et al., 1974; Szabo and Rayner, 1980). Individual rotamers are expected to be associated with a single decay time component with the preexponential amplitudes (α_i) (or fractional concentrations, c_i) reflecting their relative populations. The exact relationships between the various rotamers of the tryptophan residue, their relative populations and interconversion rates, and the recovered fluorescence parameters are not fully resolved (see Eftink, 1991; Gordon et al., 1992; Ross et al., 1992 and references cited therein). However, direct correlation between the fluorescence decay kinetics and tryptophan conformation have been established by a number of techniques. These include supersonic jet spectroscopy (Philips et al., 1988), NMR (Tilstra et al., 1990; Colucci et al., 1990; Ross et al., 1992) and protein crystal fluorescence spectroscopy (Dahms et al., 1993).

On the basis of the preceding discussion, we would therefore expect the fluorescence decay kinetics of a tryptophan residue to be sensitive to main-chain conformation and act as a probe of "local" secondary structure. This was found to be the case. The decay times, and in particular their relative contributions, observed for the central tryptophan residue in the two model peptides were well correlated with the α-helix content. The strongest feature observed was the increase in the contribution of the long decay time component and the corresponding decrease in the contribution of the intermediate decay time component, which accompanied helix formation.

According to McGregor et al., (1987) the g^+ rotamer[3] is unfavorable for TRP in an α-helix due to a clash of the C_γ atom with the carbonyl oxygen of the *i*-3 residue, the g^- rotamer results in less severe C_γ-$O_{(i-4)}$ interactions while the favored t rotamer points away from the helix with little steric hindrance (Fig. 5). The most recent crystal structure survey

[2] The C_α-C_β rotamers are defined by the angle $\chi_1 \equiv$ N-C_α-C_β-C_γ dihedral angle. The rotamers g^+, g^-, and t correspond to $\chi_1 = 60 \pm 60°$, $-60 \pm 60°$, and $180 \pm 60°$, respectively. C_β-C_γ rotamers are defined by the angle $\chi_2 \equiv$ N-C_α-C_β-C_γ-$C_{\delta 2}$ dihedral angle (IUPAC-IUB Commission on Biochemical Nomenclature, 1970).

[3] Janin et al. (1978), McGregor et al. (1987), and Schrauber et al. (1993) define g^+ and g^- opposite to the convention adopted here.

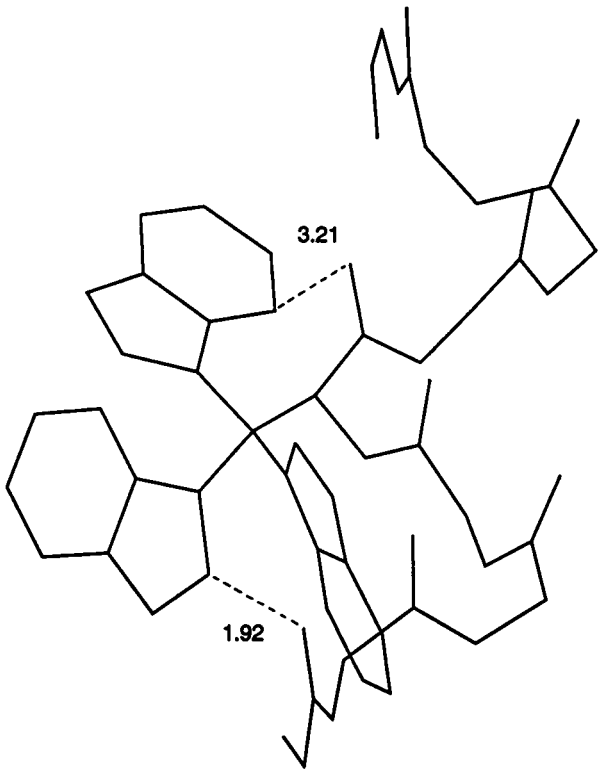

FIGURE 5 Tryptophan side-chain interactions with an α-helical main-chain. A 9-residue portion of an α-helix is shown, as is the 3 χ_1 rotamers of the central tryptophan residue side-chain (clockwise from the top; t, g^+, and g^-: $\chi_2 = -90°$). Note that the t rotamer experiences little steric hindrance, whereas the g^+ rotamer clashes with the main-chain. Interatomic distances have units of Å.

(Schrauber et al., 1993) finds the following main-chain conformation dependent fractional χ_1 rotamer frequencies, for 181 Trp residues. Average of all main-chain conformations 50% (g^-), 35% (t), 15% (g^+); β-conformation 62% (g^-), 25% (g^+), 12% (t); α-conformation 65% (t), 22% (g^-), 13% (g^+). Comparing these trends with our time-resolved fluorescence data it is tempting to associate the long decay time component with the t rotamer, since its contribution dramatically increases with helix content. Inversely, the g^- rotamer could be assigned as the intermediate decay time component, and the sterically unfavorable g^+ rotamer as the short decay time component. However, we note that this picture clearly represents an oversimplification since, for example, the role of χ_2 rotamers has not been considered and also the "true" fluorescence decay kinetics of the system are likely to be more complex that the fitted triple exponential model.

The similarity of the fluorescence decay times for the two model peptides, both the absence of any changes in the shapes of the decay associated spectra, and the lack of any dramatic changes in decay times with helical content indicates that the changes observed in the α_i or c_i values are not due to any tryptophan environmental changes resulting from different interactions with the other side chain in the helical and non-helical states. The changes in α_i and c_i values are rationalized in terms of a restructured side-chain rotamer model, and implies a linear relationship between the relative contribution of the decay times and the α-helical content. This relationship was observed for both HD and HM.[4]

The simplest model consistent with the time-resolved fluorescence data for both HD and HM, required three emission wavelength and α-helix content independent decay times. It could be argued, that the decay kinetics of a Trp residue potentially sampling at least 12 low energy conformations (e.g. 2 main chain, 3χ, and 2 χ_2 conformations), should be modeled as a continuous distribution of exponential decay times. The "width" of the recovered distribution reflecting the heterogeneity of the system under a given set of conditions (James and Ware, 1985; Alcala et al., 1987). Distribution analysis of the data for HD in both the α-helical state and at the midpoint of the transition gave fit statistics that equaled but did not exceed the quality of those obtained from discrete exponential analysis. Unfortunately the "widths" of the recovered distribution modes were poorly defined (despite employing global analysis techniques) and did not reflect the change in secondary structure.

A number of factors need to be considered in the potential application of the correlation between "local" helical main-chain conformation and Trp fluorescence decay kinetics. For example, at the primary structure level interactions with neighboring side chains ($i \pm 3$, $i \pm 4$) will likely result in a range of values for the fluorescence parameters exhibited by a Trp residue in an α-helix (Schrauber et al., 1993) and, more significantly, in the unfolded state. This probably accounts for the minor differences in the fluorescence decay times of HD and HM. It is expected that the general pattern observed for both the decay times and relative proportions of the decay components for the HD and HM will be preserved[5] in other sequences.

Specific interactions may also lead to the preferential quenching of one or more of the Trp rotamers, complicating the analysis (Chen et al., 1991). For example, according to NMR the long (2.64 ns), intermediate (1.08 ns) and short (0.32 ns) decay time components were associated with the g^+, t, and g^-, χ_1 rotamers in the 9 residue cyclic peptide [Trp^2] oxytocin (Ross et al., 1992). Both the g^- and t rotamers can interact with the disulfide bridge of the peptide. Since disulfides are efficient quenchers of Trp fluorescence, this may explain why the g^+ and t decay time class assignments are apparently reversed for this peptide (compared to HD and HM).

[4] For HD at helix contents >70%, some curvature is observed (Fig. 3). This is probably due to a contribution from higher aggregates as the [GuHCl] is reduced to zero. Association of dimers to form n-mers may also explain why the point on Fig. 1 corresponding to the highest peptide concentration measured does not lie on the theoretical curve for a monomer-dimer equilibrium.

[5] In an earlier study (Willis and Szabo, 1992) of the linear peptide parathyroid hormone 1-34, it was reported that the long decay time component of the single Trp residue showed a 10% increase in its relative contribution when the native and denatured stated were compared. Subsequent data (not shown) collected at a series of denaturant concentrations and analyzed simultaneously gave results that paralleled those reported here for HM.

At the secondary structure level it appears from the X-ray crystallography data that the non-α-helical regions of the allowed ϕ, Ψ conformational space also exhibit distinct χ_1 rotamer preferences. As discussed above, the extended β main-chain structure is expected to result in a low (ca. 10%) frequency for the t rotamer, which we have suggested is associated with the long decay time component. A high frequency (ca. 60%) is expected for the g^- rotamer associated with the intermediate decay time component. The snake neurotoxin erabutoxin b contains a single solvent exposed Trp residue in a β-sheet, and it is interesting to note that this protein displays long (3.85 ns), intermediate (1.18 ns) and short (0.26 ns) decay times with relative contributions of 10%, 80%, and 10%, respectively (Dahms et al., 1993)

Packing requirements at the tertiary structure level may constrain the Trp side-chain and in specific cases can potentially affect rotamer frequencies and displace χ_1 angles from their local minima (rotamer) values (Janin et al., 1978; Schrauber et al., 1993). This may also be important when "exposed" Trp residues are in contact with surfaces, for example in protein:protein or protein:membrane interactions.

The results in this work show that the time-resolved fluorescence properties of a Trp residue potentially report on the side-chain and main-chain conformation. We anticipate that the ability to probe the conformational properties of a specific site in a protein or peptide will be a useful tool in structural investigations. In protein folding, for example, the restriction of side-chain conformation in the α-helix may be a significant factor in determining the helix forming tendencies of amino acids (Padmanabhan et al., 1990; Lya et al., 1991; Go et al., 1992). It is often important to be able to determine the location of helical regions within peptides and the correlation's we have demonstrated here will allow fluorescence spectroscopy (Willis and Szabo, 1992) to supplement data from other spectroscopic techniques (Dyson and Wright, 1991; Liff et al., 1991).

Finally, an example of the application of approaches similar to those described here, to monitor protein unfolding, have recently been reported (Eftink and Wasylewski, 1992). The single Trp residue of *Staphylococcal* nuclease A was shown to display fluorescent decay time components whose relative contributions were conformation dependent and consistent with the correlations proposed in this work.

The technical assistance of D. T. Krajcarski is gratefully acknowledged. We also thank Dr. M. Yaguchi for performing the ESI mass spectroscopy and Dr. M. J. McGregor for helpful discussions.

Issued as NRCC Publication No. 37378. This work was partially funded by an NRC-Allelix Biopharmaceuticals Inc. Biotechnology Contribution Program.

REFERENCES

Alcala, R., E. Gratton, and F. Prendergast. 1987. Interpretation of fluorescence decays in proteins using continuous lifetime distributions. *Biophys J.* 58:587–596.

Bayley, P., and S. Martin. 1989. Analysis of complex fluorescence decay data. *In* Fluorescent Biomolecules. D. M. Jameson and G. D. Reinhart, editors. Plenum Press, New York. 389–390.

Benedetti, E., Morelli, G., Nemethy, G., and Scheraga, H. A. 1983. Statistical and energetic analysis of side-chain conformations in oligopeptides. *Int. J. Pept. Protein Res.* 22:1–15.

Bhat, T. N., Sasisekharan, V., and Vijayan, M. 1979. An analysis of side-chain conformation in proteins. *Int. J. Pept. Protein Res.* 13:170–184.

Chen, R. F., Knuston, J. R., Ziffer, H., and Porter, D. 1991. Fluorescence of tryptophan dipeptides: correlations with the rotamer model. *Biochemistry* 30:5184–5195.

Colucci, W. J., Tilstra, L. Sattler, M. C., Fronczek, F. R., and Barkley, M. D. 1990. Conformational studies of a constrained tryptophan derivative: implications for the fluorescence quenching mechanism. *J. Am. Chem. Soc.* 112:9182–9190.

Dahms, T. E. S., Willis, K. J., and Szabo, A. G. 1993. Fluorescence decay kinetics of a tryptophyl residue in a protein crystal. *Biophys J.* 64:A55.

Donzel, B., Gauduchon, P., and Wahl, Ph. 1974. Study of the conformation in the excited state of two tryptophanyl diketopiperazines. *J. Am. Chem. Soc.* 96:801–808.

Dyson, H. J. and Wright, P. E. 1991. Peptide conformation and protein folding. *Annu. Rev. Biophys. Biophys. Chem.* 20:519–538.

Eftink, M. R. 1991. Fluorescence techniques for studying protein structure. in *Methods of Biochemical Analysis Volume 35:* Protein Structure Determination (Suelter, C. H., Ed.) pp. 127–205, John Wiley, New York.

Eftink, M. R. and Wasylewski, Z. 1992. Time-resolved fluorescence studies of the thermal and guanidine induced unfolding of nuclease A and its unstable mutant. *SPIE Vol. 1640 Time-Resolved Laser Spectroscopy in Biochemistry* III:579–584.

Go, K., Chaturvedi, S., and Parthasarathy, R. 1992. Helix-forming tendencies of amino acids depend on the restrictions of side-chain rotamer conformations: crystal structure of the tripeptide GA1 in two crystalline forms. *Biopolymers* 32:107–117.

Gordon, H. L., Jarrell, H. C., Szabo, A. G., Willis, K. J., and Somorjai, R. L. 1992. Molecular dynamics simulations of the conformational dynamics of tryptophan. *J. Phys. Chem.* 96:1915–1921.

IUPAC-IUB Commission on Biochemical Nomenclature 1970. *Biochemistry* 9:3471–3479.

James, D. R. and Ware, W. R. 1985. A fallacy in the interpretation of fluorescence decay parameters. *Chem. Phys. Lett.* 120:450–454.

Janin, J., Wodak, S., Levitt, M., and Maigrett, B. 1978. Conformation of amino acid side-chains in proteins. *J. Mol. Biol.* 125:357–386.

Knutson, J. R., Beechem, J. M., and Brand, L. 1983. Simultaneous analysis of multiple fluorescence decay curves: a global approach. *Chem. Phys. Lett.* 102:501–507.

Knutson, J. R., Walbridge, D. G. and Brand, L. 1982. Decay-associated fluorescence spectra and the heterogeneous emission of alcohol dehydrogenase. *Biochemistry* 21:4671–4679.

Krimm, S., and Bandekar, J. 1986. Vibrational spectroscopy and conformation of peptides, polypeptides, and proteins. *Adv. Protein Chem.* 38: 181–364.

Liff, M. I., Lyu, P. C., and Kallenbach, N. R. 1991. Analysis of asymmetry in the distribution of helical residues in peptides by ^1H nuclear magnetic resonance. *J. Am. Chem. Soc.* 113:1014–1019.

Lyu, P., Sherman, J. C., Chen, A., and Kallenbach, N. R. 1991. α-Helix stabilization by natural and unnatural amino acids with alkyl side chains. *Proc. Natl. Acad. Sci. USA* 88:5317–5320.

Marqusee, S., and Baldwin, R. L. 1987. Helix stabilization by Glu^- Lys^+ salt bridges in short peptides of de novo design. *Proc. Natl. Acad. Sci. USA.* 84:8898–8902.

McGregor, M. J., Islam, S. A., and Sternberg, M. J. E. 1987. Analysis of the relationship between side-chain conformation and secondary structure in globular proteins. *J. Mol. Biol.* 198:295–310.

Mei, G., Rosato, N., Silva, N., Rusch, R., Gratton, E., Savinin, I., and Finazzi-Agrò, A. 1992. Denaturation of human Cu/Zn superoxide dismutase by guanidine hydrochloride: a dynamic fluorescence study. *Biochemistry* 31:7224–7230.

Merutka, G., Lipton, W., Shalongo, W., Park, S.-H., and Stellwagen, E. 1990. Effect of central-residue replacements on the helical stability of a monomeric peptide. *Biochemistry* 29:7511–7515.

Merutka, G., Shalongo, W., and Stellwagen, E. 1991. A model peptide with enhanced helicity. *Biochemistry* 30:4245–4248.

Merutka, G., and Stellwagen, E. 1991. Effect of amino acid ion pairs on peptide helicity. *Biochemistry* 30:1591–1594.

O'Neil, K. T., and DeGrado, W. F. 1990. A thermodynamic scale for the helix-forming tendencies of the commonly occurring amino acids. *Science* 250:646–651.

Padmanabhan, S., Marqusee, S., Ridgeway, T., Laue, T. M., and Baldwin, R. L. 1990. Relative helix-forming tendencies of nonpolar amino acids. *Nature* 344:268–270.

Philips, L. A., Webb, S. P., Martinez, S. J., III, Fleming, G. R., and Levy, D. H. 1988. Time-resolved spectroscopy of tryptophan conformers in a supersonic jet. *J. Am. Chem. Soc.* 110:1352–1355.

Piela, L., Nemethy, G., and Scheraga, H. A. 1987. Conformational constraints of amino acid side chains in α-helices. *Biopolymers* 26:1273–1286.

Ponder, J. W., and Richards, F. M. 1987. Tertiary templates for proteins use of packing criteria in the enumeration of allowed sequences for different structural classes. *J. Mol. Biol.* 193:775–791.

Ross, J. B. A., Wyssbrod, H. R., Porter, R. A., Schwartz, G. P., Michaels, C. A. and Laws, W. R. 1992. Correlation of tryptophan fluorescence intensity decay parameters with ^{1}H NMR-determined rotamer conformations: [tryptophan^2]oxytocin. *Biochemistry.* 31:1585–1594.

Scholtz, J. M. and Baldwin, R. L. 1992. The mechanism of α-helix formation by peptides. *Annu. Rev. Biophys. Biomol. Struct.* 21:95–118.

Schrauber, H., Eisenhaber, F., and Argos, P. 1993. Rotamers: to be or not to be? An analysis of amino acid side-chain conformations in globular proteins. *J. Mol. Biol.* 230:592–612.

Szabo, A. G. and Rayner, D. M. 1980. Fluorescence decay of tryptophan conformers in aqueous solution. *J. Am. Chem. Soc.* 102:554–563.

Tadesse, L., Nazarbaghi, R., and Walters, L. 1991. Isotopically enhanced infrared spectroscopy: a novel method for examining secondary structure at specific sites in conformationally heterogeneous peptides. *J. Am. Chem. Soc.* 113:7036–7037.

Tilstra, L., Sattler, M. C., Cherry, W. R., and Barkley, M. D. 1990. Fluorescence of a rotationally constrained tryptophan derivative, 3-carboxy-1,2,3,4-tetrahydro-2-carboline. *J. Am. Chem. Soc.* 112:9176–9182.

Willis, K. J., Szabo, A. G. and Krajcarski, D. T. 1990a. The use of stokes raman scattering in time correlated single photon counting: application to the fluorescence lifetime of tyrosinate. *Photochem. Photobiol.* 51: 375–377.

Willis, K. J., Szabo, A. G., Zuker, M., Ridgeway, J. M., and Alpert, B. 1990b. Fluorescence decay kinetics of the tryptophyl residues of myoglobin: effect of heme ligation and evidence for discrete lifetime components. *Biochemistry* 29:5270–5275.

Willis, K. J. and Szabo, A. G. 1992. Conformation of parathyroid hormone: time-resolved fluorescence studies. *Biochemistry* 31:8924–8931.

Willis, K. J. and Szabo, A. G. 1989. Resolution of tyrosyl and tryptophyl fluorescence emission from subtilisins. *Biochemistry* 28:4902–4908.

Woody, R. W. 1985. Circular dichroism of peptides. *The Peptides* 7:15–114.